Frequency-Domain Channel Estimation and Equalization for Single Carrier Underwater Acoustic Communications

Yahong Rosa Zheng[§], Chengshan Xiao[§], T. C. Yang[†] and Wen-Bin Yang[†]

[§]Dept. of Electrical & Computer Eng., University of Missouri-Rolla, MO 65409
[†]Naval Research Laboratory, Washington, DC 20375

***Abstract*— A new frequency-domain channel estimation and equalization (FDE) scheme is proposed for single carrier (SC) underwater acoustic communications. The proposed SC-FDE employs a small training signal block for initial channel estimation in the frequency domain and converts the estimated transfer function to a desired DFT (discrete Fourier transform) size for channel equalization of the data blocks. The frequency domain equalizer is designed using the linear minimum mean square error criterion. A new phase coherent detection scheme is also proposed and deployed to combat the phase drift due to the instantaneous Doppler in the underwater channels. The channel transfer functions and group-averaged phase drift are re-estimated adaptively in a decision-directed manner for each data block in a packet, which contains M blocks of QPSK data. The proposed SC-FDE method is applied to single input multiple output (SIMO) systems using the experimental data measured off the coast of Panama City, Florida, USA, June 2007. The uncoded bit error rate of the SIMO systems varies between 1.3% to 6.8×10^{-5} when $4 \sim 8$ receive hydrophones are utilized, and the source-receiver range is 5.06 km.**

I. Introduction

Shallow water horizontal communication channels are often hostile for high data rate underwater communications due to two major obstacles. One is the excessive multipath delay spread in a medium range shallow water channel which is usually on the order of 10–30 ms and causes the intersymbol interference (ISI) to extend over 20-300 symbols at a data rate of 2-10 kilosymbols per second. Another obstacle is the time-varying Doppler shift due to relative motion between the source (transducers) and receiver (hydrophones), dynamic motion of water mass, and varying sound speed, etc. A few Hz of Doppler in underwater channels can be very significant due to the low velocity of acoustic waves ($\sim$1500 m/s). The ratio of Doppler to carrier frequency in underwater channels is on the order of 10^{-3} to 10^{-4}; while the ratio in RF wireless channels is on the order of 10^{-7} to 10^{-9}. The significant Doppler shift cause not only rapid fluctuation in the fading channel response but also compression or dilation of signal waveforms. These two obstacles make the coherent receiver of underwater communication systems much more complex [1]-[4] than RF systems.

It has been successfully demonstrated in [1] that coherent detection of underwater acoustic communications can be realized by joint decision feedback equalization (DFE) and phase synchronization that employs a phase-locked loop (PLL) or delay-locked loop (DLL). However, the DFE and PLL/DLL have to interact in a nonlinear fashion and in a symbol-by-symbol basis, therefore it requires careful selection of the number of equalizer taps and tuning of the equalizer and PLL/DLL coefficients. Stable and robust operation of the time-domain equalizer is sometimes difficult to obtain in different channel conditions. Recent improvement on robust time-domain DFE has been reported in [4] using a fixed set of parameters at a cost of slightly degraded bit error performance.

Further increasing of data rates imposes a greater challenge on time-domain coherence receivers. Therefore, orthogonal frequency division multiplex (OFDM) techniques have been applied to underwater acoustic channels [5], [6] with some promising results. Adaptive channel and phase estimation was used in [5] to update the channel Doppler and carrier frequency offset (CFO) from block to block and secure successful data detection. In [6], carrier frequency offset and channel estimation were performed within each OFDM block employing 25% of the OFDM bandwidth for pilot tones and 75% for payload. Therefore it is suitable for fast varying channels provided that the frequency selective channel length is less than the number of pilot tones. Both algorithms employ quadrature phase shift keying (QPSK) and assume constant Doppler shift and/or carrier frequency offset (CFO) over one OFDM block. It has been shown by field data measurements that the OFDM schemes are successful for block sizes up to 1024 data symbols.

Alternative to the OFDM approach, a single carrier system with frequency-domain equalization (SC-FDE) has been shown [7], [8] to have comparable performance and complexity for RF broadband wireless communications. Besides, SC-FDE has the advantage of lower peak-to-average power ratio and less sensitivity to carrier frequency offsets. Compared to time-domain equalization, SC-FDE has better convergence properties [9] and less computational complexity in severe inter-symbol interferences (ISI) channels. However, the SC-FDE schemes developed for broadband RF uplink communication systems may not be applied directly to underwater channels.

In this paper, we propose a new frequency-domain channel estimation and equalization scheme for single carrier underwater acoustic communications. The proposed SC-FDE employs a small training signal block for initial channel estimation in the frequency domain and converts the estimated transfer function to a desired DFT (discrete Fourier transform) size for channel equalization of the data blocks. The frequency domain

0-933957-35-1 ©2007 MTS

Report Documentation Page

Form Approved
OMB No. 0704-0188

Public reporting burden for the collection of information is estimated to average 1 hour per response, including the time for reviewing instructions, searching existing data sources, gathering and maintaining the data needed, and completing and reviewing the collection of information. Send comments regarding this burden estimate or any other aspect of this collection of information, including suggestions for reducing this burden, to Washington Headquarters Services, Directorate for Information Operations and Reports, 1215 Jefferson Davis Highway, Suite 1204, Arlington VA 22202-4302. Respondents should be aware that notwithstanding any other provision of law, no person shall be subject to a penalty for failing to comply with a collection of information if it does not display a currently valid OMB control number.

1. REPORT DATE **SEP 2007**	2. REPORT TYPE	3. DATES COVERED **00-00-2007 to 00-00-2007**
4. TITLE AND SUBTITLE **Frequency-Domain Channel Estimation and Equalization for Single Carrier Underwater Acoustic Communications**		5a. CONTRACT NUMBER 5b. GRANT NUMBER 5c. PROGRAM ELEMENT NUMBER
6. AUTHOR(S)		5d. PROJECT NUMBER 5e. TASK NUMBER 5f. WORK UNIT NUMBER
7. PERFORMING ORGANIZATION NAME(S) AND ADDRESS(ES) **University of Missouri-Rolla,Dept. of Electrical & Computer Eng,Missouri-Rolla,MO,20375**		8. PERFORMING ORGANIZATION REPORT NUMBER
9. SPONSORING/MONITORING AGENCY NAME(S) AND ADDRESS(ES)		10. SPONSOR/MONITOR'S ACRONYM(S) 11. SPONSOR/MONITOR'S REPORT NUMBER(S)

12. DISTRIBUTION/AVAILABILITY STATEMENT
Approved for public release; distribution unlimited

13. SUPPLEMENTARY NOTES
See also ADM002047. Presented at the MTS/IEEE Oceans 2007 Conference held in Vancouver, Canada on Sep 29-Oct 4, 2007. U.S. Government or Federal Purpose Rights License.

14. ABSTRACT
See Report

15. SUBJECT TERMS

16. SECURITY CLASSIFICATION OF:			17. LIMITATION OF ABSTRACT	18. NUMBER OF PAGES	19a. NAME OF RESPONSIBLE PERSON
a. REPORT **unclassified**	b. ABSTRACT **unclassified**	c. THIS PAGE **unclassified**	**Same as Report (SAR)**	**6**	

Standard Form 298 (Rev. 8-98)
Prescribed by ANSI Std Z39-18

equalizer is designed using the linear Minimum Mean Square Error (MMSE) criterion. A new phase coherent detection scheme is then developed to combat the phase drift due to the instantaneous Doppler in the underwater channels. The channel transfer functions and group-averaged phase drift are re-estimated adaptively in a decision-directed manner for each data block of a packet, which contains M blocks of QPSK data. The proposed SC-FDE method is applied to SIMO systems using the experimental data measured off the coast at Panama City, Florida, USA in June 2007. The uncoded bit error rate of the SIMO systems varies between 1.3% to 6.8×10^{-5} when $4 \sim 8$ receive hydrophones are utilized, and the source-receive range is 5.06 km.

The advantages of the proposed SC-FDE scheme are two folds. First, the size of the training signal block can be different from the DFT size. As long as it covers the fading channel length, it can be selected small to reduce the overhead. Second, the new phase correction scheme operates on averaged-group phase drift rather than individual symbol's phase thus providing robustness against noise and interference.

This paper also presents a generic channel model for SISO and SIMO underwater acoustic communication systems. A rigorous derivation of the proposed SC-FDE is then developed based on the model and the mathematical formulas provide theoretical support and insightful understanding on how the method achieves the high performance.

II. The System Model and Preliminaries

Consider a underwater acoustic communications system using a single transducer source and M-hydrophone receiver. The baseband equivalent signal received at the m-th hydrophone can be expressed in discrete-time domain as

$$y_m(k) = \sum_{l=1}^{L} h_m(l,k) x(k+1-l) e^{j(2\pi f_{m,k} kT + \theta_{m,0})} + v_m(k) \quad (1)$$

where

k	time index;
$y_m(k)$	received signal sample;
$x(k)$	transmitted data symbol or pilot symbol;
$h_m(l,k)$	impulse response of the frequency-selective, time-varying fading channel with length L;
L	fading channel length in terms of T;
T	data symbol interval;
$f_{m,k}$	time-varying carrier frequency offset (CFO) or instantaneous Doppler shift caused by relative motion between the transducer and hydrophone, dynamic motion of water mass, varying sound speed, and changing water columns, etc.;
$\theta_{m,0}$	phase error after coarse synchronization;
$v_m(k)$	white Gaussian noise with average power σ^2.

If the Doppler shift $f_{m,k}$ is significant, then it causes the received signal $y_m(k)$ to be time-scaled (compressed or dilated) signal [2], [10]. In this case, re-scaling and re-sampling are required before equalization taking place to cancel ISI. If the relative motion between the source and receiver is insignificant, then the average Doppler shift $E\{f_{m,k}\}$ is close to zero, but the instantaneous Doppler $f_{m,k}$ is a time-varying random variable with a zero mean. In this paper, we focus on the case where the source and receiver are stationary with $E\{f_{m,k}\} = 0$. The case with $E\{f_{m,0}\} \neq 0$ will be considered in our future work.

It is noted that the fading coefficients $h_m(l,k)$ include the effects of the transmit pulse-shape filter, physical multipath fading channel response, and the receive matched filter. It is found that the fading channel coefficients usually change much slower than the instantaneous phase $2\pi f_{m,k} kT$ in many practical underwater acoustic channels [1], [3]. That is the main reason to explicitly separate the phase $2\pi f_{m,k} kT$ from the fading coefficients $h_m(l,k)$ in (1).

To facilitate frequency-domain channel estimation and equalization for the system described in (1), the transmitted data sequence $\{x(k)\}$ are partitioned into blocks of size N. Each block is then added with N_{zp} cyclic prefix or padded with N_{zp} zeros [9]. For the zero-padding scheme, a transmission block is

$$\mathbf{x}^{bk} = \begin{bmatrix} x(1) & x(2) & \cdots & x(N) & 0 & \cdots & 0 \end{bmatrix}^t \quad (2)$$

The corresponding received signal $\mathbf{y}_m^{bk}$ of the block is denoted by

$$\mathbf{y}_m^{bk} = \begin{bmatrix} y(1) & y(2) & \cdots & y(N) & \cdots & y(N+N_{zp}) \end{bmatrix}^t \quad (3)$$

where the superscript $[\cdot]^t$ is the transpose. The length of zero padding N_{zp} is chosen to be at least $L-1$ so that the inter-block interference is avoided in the received signal.

Adopting the overlap-add method [11] for N-point DFT, we define two signal vectors

$$\mathbf{x} = \begin{bmatrix} x(1) & x(2) & \cdots & x(N) \end{bmatrix}^t \quad (4)$$

$$\mathbf{y}_m = \begin{bmatrix} y_m(1) & \cdots & y_m(N_{zp}) & y_m(N_{zp}+1) & \cdots & y_m(N) \end{bmatrix}^t + \begin{bmatrix} y_m(N+1) & \cdots & y_m(N+N_{zp}) & 0 & \cdots & 0 \end{bmatrix}^t \quad (5)$$

and their corresponding frequency-domain signals $\mathbf{Y}_m \triangleq \mathbf{F}_N \mathbf{y}_m$ and $\mathbf{X} \triangleq \mathbf{F}_N \mathbf{x}$, where $\mathbf{F}_N$ is the normalized DFT matrix of size $N \times N$, *i.e.*, its (m,n)-th element is given by $\frac{1}{\sqrt{N}} \exp\left(\frac{-j2\pi(m-1)(n-1)}{N}\right)$. Note that $\mathbf{F}_N^h \mathbf{F}_N = \mathbf{I}_N$.

The time-domain signals $\mathbf{x}$ and $\mathbf{y}_m$ are related as

$$\mathbf{y}_m = \mathbf{T}_m \mathbf{D}_m \mathbf{x} + \mathbf{v}_m \quad (6)$$

with

$$\mathbf{T}_m = \begin{bmatrix} h_m(1,1) & 0 & \cdots & 0 & h_m(L,1) & \cdots & h_m(2,1) \\ h_m(2,2) & h_m(1,2) & 0 & \ddots & \ddots & \ddots & \vdots \\ \vdots & \ddots & \ddots & \ddots & \ddots & \ddots & h_m(L,L-1) \\ h_m(L,L) & \ddots & \ddots & h_m(1,L) & 0 & \ddots & 0 \\ 0 & h_m(L,L+1) & \ddots & \ddots & \ddots & \ddots & \vdots \\ \vdots & \ddots & \ddots & \ddots & \ddots & \ddots & 0 \\ 0 & \cdots & 0 & h_m(L,N) & \cdots & \cdots & h_m(1,N) \end{bmatrix} \quad (7)$$

$$\mathbf{D}_m = \text{diag}\left\{ e^{j(2\pi f_{m,1}T+\theta_{m,0})} \quad \cdots \quad e^{j(2\pi f_{m,N}NT+\theta_{m,0})} \right\} \quad (8)$$

$$\mathbf{v}_m = \left[v_m(1) \ \cdots \ v_m(N_{zp}) \ v_m(N_{zp}+1) \ \cdots \ v_m(N) \right]^t + \left[v_m(N+1) \ \cdots \ v_m(N+N_{zp}) \ 0 \ \cdots \ 0 \right]^t. \quad (9)$$

The frequency-domain representation is

$$\begin{aligned} \mathbf{Y}_m &= \mathbf{F}_N \mathbf{T}_m \mathbf{F}_N^h \mathbf{F}_N \mathbf{D}_m \mathbf{F}_N^h \mathbf{F}_N \mathbf{x} + \mathbf{F}_N \mathbf{v}_m \\ &= \mathbf{H}_m \mathbf{\Phi}_m \mathbf{X} + \mathbf{V}_m \end{aligned} \quad (10)$$

where $\mathbf{H}_m = \mathbf{F}_N \mathbf{T}_m \mathbf{F}_N^h$ is the frequency-domain channel matrix (or channel transfer function matrix) for the block, and $\mathbf{\Phi}_m = \mathbf{F}_N \mathbf{D}_m \mathbf{F}_N^h$ the frequency-domain Doppler and phase matrix for the block.

Although $\mathbf{\Phi}_m$ is generally a non-diagonal matrix, its diagonal elements, $\{\Phi_m(n,n)\}_{n=1}^N$ are identical and equal to

$$\Phi_m(n,n) = \frac{1}{N} \sum_{k=1}^{N} e^{j(2\pi f_{m,k} kT+\theta_{m,0})}, \quad n = 1, 2, \cdots, N. \quad (11)$$

This property of the single-carrier frequency-domain representation enables effective channel estimation and equalization.

III. Frequency-Domain Channel Estimation

In the channel estimation mode, a small block of N_{ts} training symbols are padded with N_{zp} zeros ($N_{zp} < N_{ts}$) and transmitted over the acoustic channel. We choose the number of training symbols N_{ts} such that the training block time duration $(N_{ts} + N_{zp})T$ is smaller than a third of the channel coherence time. Therefore, the non-diagonal elements of $\mathbf{\Phi}_m$, *i.e.*, $\Phi_m(n,l)$ with $n \neq l$, are negligible comparing to the diagonal elements $\Phi_m(n,n)$. Moreover, the fading channel coefficients remain constant for the entire training block, thus the time-domain channel matrix $\mathbf{T}_m$ becomes a circulant matrix and the frequency-domain channel matrix $\mathbf{H}_m$ becomes a diagonal matrix. That is, $\mathbf{H}_m$=diag $\{H_m(1), \quad H_m(2), \quad \cdots, \quad H_m(N_{ts})\}$ with $H_m(n) = \sum_{l=1}^{L} h_m(l,1) \exp\left(\frac{-j2\pi(l-1)(n-1)}{N_{ts}}\right)$. Therefore, the frequency-domain representation (10) can be simplified as

$$\begin{aligned} Y_m(n) &= H_m(n)\Phi_m(n,n)X(n) + V_m(n) \\ &= \lambda_m H_m(n) X(n) + V_m(n), \ n = 1, 2, \cdots, N_p \end{aligned} \quad (12)$$

where $\lambda_m = \frac{1}{N_{ts}} \sum_{k=1}^{N_{ts}} e^{j(2\pi f_{m,k}T+\theta_{m,0})}$, is a complex-valued unknown parameter with amplitude close to unit.

The channel transfer function $\lambda_m H_m(n)$ is estimated by the least squares criterion as

$$\lambda_m \tilde{H}_m(n) = \frac{Y_m(n)}{X(n)}, \quad n = 1, 2, \cdots, N_{ts}. \quad (13)$$

The estimate $\lambda_m \tilde{H}_m(n)$ can be further improved by a frequency-domain filter to reduce noise

$$\lambda_m \breve{\mathbf{H}}_m = \lambda_m \mathbf{F}_{N_{ts}}[1:N_{zp}] \left(\mathbf{F}_{N_{ts}}[1:N_{zp}]\right)^h \tilde{\mathbf{H}}_m \quad (14)$$

where $\mathbf{F}_{N_{ts}}[1:N_{zp}]$ denotes the first N_{zp} columns of $\mathbf{F}_{N_{ts}}$, $\breve{\mathbf{H}}_m = \text{diag}\left\{ \breve{H}_m(1) \quad \breve{H}_m(2) \quad \cdots \quad \breve{H}_m(N_{ts}) \right\}$, and $\tilde{\mathbf{H}}_m = \text{diag}\left\{ \tilde{H}_m(1) \quad \tilde{H}_m(2) \quad \cdots \quad \tilde{H}_m(N_{ts}) \right\}$.

The N_{ts}-point transfer function $\lambda_m \breve{\mathbf{H}}_m$ can be directly transformed into an N-point transfer function by

$$\lambda_m \hat{\mathbf{H}}_m = \lambda_m \mathbf{F}_N[1:N_{zp}] \left(\mathbf{F}_{N_{ts}}[1:N_{zp}]\right)^h \tilde{\mathbf{H}}_m \quad (15)$$

where $\mathbf{F}_N[1 : N_{zp}]$ denotes the first N_{zp} columns of $\mathbf{F}_N$ (the N-point DFT matrix) and $\hat{\mathbf{H}}_m = \text{diag}\left\{ \hat{H}_m(1) \quad \hat{H}_m(2) \quad \cdots \quad \hat{H}_m(N) \right\}$. The estimated N-point transfer function is then used for frequency-domain channel equalization which is detailed in the next section.

IV. Frequency-Domain Channel Equalization

In the data transmission mode, we choose the data block time duration $(N+N_{zp})T$ slightly smaller than the channel coherence time, therefore the frequency-domain channel matrices of all M hydrophones $\{\mathbf{H}_m\}_{m=1}^M$ are diagonal matrices. Based on (10), a block of the received signals at the M hydrophones can be expressed in the frequency domain as

$$\begin{bmatrix} \mathbf{Y}_1 \\ \mathbf{Y}_2 \\ \vdots \\ \mathbf{Y}_M \end{bmatrix} = \begin{bmatrix} \mathbf{H}_1 \mathbf{\Phi}_1 \\ \mathbf{H}_2 \mathbf{\Phi}_2 \\ \vdots \\ \mathbf{H}_M \mathbf{\Phi}_M \end{bmatrix} \mathbf{X} + \begin{bmatrix} \mathbf{V}_1 \\ \mathbf{V}_2 \\ \vdots \\ \mathbf{V}_M \end{bmatrix}. \quad (16)$$

The training block is utilized to estimate the channel transfer function matrices $\{\lambda_m \hat{\mathbf{H}}_m\}_{m=1}^M$ and these are used to equalize the first data block. Applying the MMSE criterion, we obtain the frequency-domain equalized block data as

$$\begin{aligned} \hat{\mathbf{X}} &= \left(\sum_{m=1}^{M} |\lambda_m|^2 \hat{\mathbf{H}}_m^h \hat{\mathbf{H}}_m + \sigma^2 \mathbf{I}_N \right)^{-1} \left(\sum_{m=1}^{M} \lambda_m^* \hat{\mathbf{H}}_m^h \mathbf{Y}_m \right) + \hat{\mathbf{V}} \\ &= \left(\sum_{m=1}^{M} |\lambda_m|^2 \hat{\mathbf{H}}_m^h \hat{\mathbf{H}}_m + \sigma^2 \mathbf{I}_N \right)^{-1} \left(\sum_{m=1}^{M} \lambda_m^* \hat{\mathbf{H}}_m^h \mathbf{H}_m \mathbf{\Phi}_m \right) \mathbf{X} + \hat{\mathbf{V}} \\ &= \left(\sum_{m=1}^{M} \mathbf{\Delta}_m \mathbf{\Phi}_m \right) \mathbf{X} + \hat{\mathbf{V}} \end{aligned} \quad (17)$$

where

$$\mathbf{\Delta}_m = \left(\sum_{m=1}^{M} |\lambda_m|^2 \hat{\mathbf{H}}_m^h \hat{\mathbf{H}}_m + \sigma^2 \mathbf{I}_N \right)^{-1} \left(\lambda_m^* \hat{\mathbf{H}}_m^h \mathbf{H}_m \right) \quad (18)$$

is a diagonal matrix due to the diagonal properties of $\{\hat{\mathbf{H}}_m\}_{m=1}^M$ and $\{\mathbf{H}_m\}_{m=1}^M$.

Applying inverse DFT to the equalized data vector $\hat{\mathbf{X}}$, we have the time-domain data vector $\hat{\mathbf{x}}$ given by

$$\begin{aligned} \hat{\mathbf{x}} &= \mathbf{F}_N^h \hat{\mathbf{X}} = \sum_{m=1}^{M} \mathbf{F}_N^h \mathbf{\Delta}_m \mathbf{\Phi}_m \mathbf{X} + \mathbf{F}_N^h \hat{\mathbf{V}} \\ &= \sum_{m=1}^{M} \mathbf{F}_N^h \mathbf{\Delta}_m \left(\mathbf{F}_N \mathbf{D}_m \mathbf{F}_N^h \right) \left(\mathbf{F}_N \mathbf{x} \right) + \hat{\mathbf{v}} \\ &= \sum_{m=1}^{M} \left(\mathbf{F}_N^h \mathbf{\Delta}_m \mathbf{F}_N \right) \mathbf{D}_m \mathbf{x} + \hat{\mathbf{v}}. \end{aligned} \quad (19)$$

Since $\mathbf{\Delta}_m$ is a diagonal matrix, all the diagonal elements of $\left(\mathbf{F}_N^h \mathbf{\Delta}_m \mathbf{F}_N\right)$ are identical and equal to $\gamma_m = \frac{1}{N}\text{trace}\left(\mathbf{\Delta}_m\right)$. When the data block time duration is less than the channel

coherence time, all the non-diagonal elements of $\left(\mathbf{F}_N^h \mathbf{\Delta}_m \mathbf{F}_N\right)$ are insignificant comparing to γ_m. Therefore, the k-th symbol of $\hat{\mathbf{x}}$ can be expressed by

$$\begin{aligned}\hat{x}(k) = & \left[\sum_{m=1}^{M} \gamma_m e^{j\left(2\pi f_{m,k} kT + \theta_{m,0}\right)}\right] x(k) + \hat{v}(k) \\ = & \left|\beta_k\right| e^{j\angle\beta_k} x(k) + \hat{v}(k)\end{aligned} \tag{20}$$

where $\beta_k = \sum_{m=1}^{M} \gamma_m e^{j\left(2\pi f_{m,k} kT + \theta_{m,0}\right)}$.

From (20), we can conclude that the complex-valued symbol-wise scaling factor β_k is actually a diversity combining factor determined by the M channel transfer functions, time-varying Doppler and timing-error phases. In other words, the equalized data symbol $\hat{x}(k)$ is an amplitude-scaled and phase-rotated version of the transmitted data symbol $x(k)$. The rotating phase $\angle\beta_k$ is a collection of all the contributions from the instantaneous Doppler $f_{m,k}$ and timing-error phases $\theta_{m,0}$ of all the M fading channels. For each individual fading channel, the rotating phase $\angle\beta_{m,k} = 2\pi f_{m,k} kT + \theta_{m,0} + \angle\gamma_m$, which represents the m-th channel's Doppler-driven shifting phase, timing-error phase, and the channel transfer function effect. This is certainly a clear physical interpretation for the single carrier frequency-domain equalized data.

To equalize the next block of data, the channel transfer function matrices need to be re-estimated using the detected data and received signals of the current block, then employ these estimated transfer function matrices to equalize the next data block. This scheme is commonly referred to as decision-directed scheme. Details are omitted here for brevity.

If $x(k)$ is phase shift keying (PSK) modulated data, then the time-varying rotating phase $\angle\beta_k$ must be compensated at the receiver after FDE and before demodulation and detection. This is discussed in detail in the next section.

V. Phase-Coherent Detection

In this section, we present a new algorithm for estimating the phase $\angle\beta_k$, which is crucial for successful data detection of PSK modulated symbols. The challenge of this phase estimation is that we face to M fading channels, in which each individual channel has different timing-error phase and time-varying Doppler, and the rotating phase $\angle\beta_k$ represents a nonlinearly composed effect of these random (or time-varying) factors of all the M fading channels. Therefore, directly estimating these Doppler and timing-error phases will be very costly if any possible.

In the literature of underwater acoustic communications, phase tracking is commonly carried out by utilizing first-order or second-order phase-locked loop or delay-locked loop [1],[3], and it is often jointly done with decision feedback equalizers. However, this approach is usually sensitive to channel conditions [4] and noise.

What we know from the nature of ocean waters is that the instantaneous Doppler $f_{m,k}$ changes gradually from time to time, *i.e.*, it does not change arbitrary in a short period of time. Therefore, the rotating phase $\angle\beta_k$ is also changing gradually from time to time. We treat $\angle\beta_k$ to be a constant for a small number of N_s consecutive received symbols, and to another constant in the next N_s consecutive received symbols, and so on so forth.

We partition the equalized N-symbol block data $\hat{\mathbf{x}}$ into N_g groups, each with N_s data symbols, except for the last group might have less than N_s symbols if N/N_g is not an integer.

Let ψ_p denote the estimated average rotating phase for the p-th group of $\{\angle\beta_{(p-1)N_s+1}, \angle\beta_{(p-1)N_s+2}, \cdots, \angle\beta_{(p-1)N_s+N_s}\}$, with $p = 1, 2, \cdots, N_g$, and let ψ_0 denote the initial rotating phase, $\Delta\psi_p$ the phase difference $\psi_p - \psi_{p-1}$. Hence

$$\psi_p = \psi_{p-1} + \Delta\psi_p, \qquad p = 1, 2, \cdots, N_g. \tag{21}$$

For MPSK modulation with symbols taken from an M-ary constellation $\mathcal{A}_{\mathcal{M}} \triangleq \left\{\exp\left[\frac{j(m-1)2\pi}{M_m}\right], m = 1, 2, \cdots, M_m\right\}$, we define a phase quantization function $\mathbb{Q}[\phi]$ as follows

$$\mathbb{Q}[\phi] = \frac{(m-1)2\pi}{M_m}, \qquad \begin{array}{c}\frac{m2\pi-3\pi}{M_m} < \phi \le \frac{m2\pi-\pi}{M_m} \\ m = 1, 2, \cdots, M_m.\end{array} \tag{22}$$

We are now in a position to present our algorithm as follows:

Algorithm: Group-wise Rotating Phase Estimation

Step 1. Designate the first N_p symbols $\{x(k)\}_{k=1}^{N_p}$ of each transmitted block data $\mathbf{x}$ as pilot symbols for phase reference to determine the initial rotating phase ψ_0 given by

$$\psi_0 = \frac{1}{N_p} \sum_{k=1}^{N_p} \angle\hat{x}(k) - \angle x(k). \tag{23}$$

Compensate the phase of the first group data by $e^{-j\psi_0}$, yielding

$$\tilde{x}_1(k) = \hat{x}(k) e^{-j\psi_0}, \qquad k = 1, 2, \cdots, N_s. \tag{24}$$

Calculate the individual phase deviation from its nominal phase of each symbol in the first group

$$\varphi_{1,k} = \angle\tilde{x}_1(k) - \mathbb{Q}\left[\angle\tilde{x}_1(k)\right], \qquad k = 1, 2, \cdots, N_s. \tag{25}$$

Calculate the average phase deviation and compute the rotating phase for the first group as follows

$$\Delta\psi_1 = \frac{1}{N_s} \sum_{k=1}^{N_s} \varphi_{1,k} \tag{26}$$

$$\psi_1 = \psi_0 + \Delta\psi_1. \tag{27}$$

Set $p = 2$ for next step.

Step 2. Compensate the phase of the p-th group data by $e^{-j\psi_{p-1}}$, yielding

$$\tilde{x}_p(k) = \hat{x}((p-1)N_s + k) e^{-j\psi_{p-1}}, \quad k = 1, 2, \cdots, N_s. \tag{28}$$

Calculate the individual phase deviation from its nominal phase of each symbol in the p-th group

$$\varphi_{p,k} = \angle\tilde{x}_p(k) - \mathbb{Q}\left[\angle\tilde{x}_p(k)\right], \qquad k = 1, 2, \cdots, N_s. \tag{29}$$

Calculate the average phase deviation and estimate the rotating phase for the p-th group as below

$$\Delta\psi_p = \frac{1}{N_s}\sum_{k=1}^{N_s}\varphi_{p,k} \tag{30}$$

$$\psi_p = \psi_{p-1} + \Delta\psi_p. \tag{31}$$

Step 3. Update $p = p + 1$, repeat Step 2 until $p = N_g$. □

After estimating the N_g group phases, we can compensate the phase rotation of the equalized data $\hat{x}$ in group basis:

$$\check{x}_p(k) = \hat{x}((p-1)N_s+k)e^{-j\psi_p}, \quad \begin{array}{c} k = 1, 2, \cdots, N_s \\ p = 1, 2, \cdots, N_g \end{array}. \tag{32}$$

Finally, the binary information data of the block can be obtained via standard MPSK demodulation procedure on the phase-compensated signal $\check{x}_p(k)$ of the block. Next block data can be processed in a similar manner, details are omitted here for brevity.

We would like to make a few remarks before leaving this section.

Remark 1: The choice of N_s symbols in a group needs to satisfy the condition: $2\pi\,|f_d|\,N_sT < \frac{\pi}{M}$, to ensure that the maximum rotating phase does not exceed a decision region of MPSK, where $|f_d|$ is the absolute value of the maximum possible Doppler.

Remark 2: The group-wise estimation of the rotating phase is insensitive to noise perturbations due to its averaging process (30), which is an implicit low-pass filtering process.

Remark 3: The equivalent composite Doppler for the M channels at p-th group can be approximated by $f_{d,p} = \frac{\Delta\psi_p}{2\pi N_s T}$.

VI. Experimental Results

In this section, we present results of the proposed frequency-domain channel estimation and equalization using experimental data. The data were collected off the coast at Panama City, Florida, USA, in June 2007. Eight hydrophones were arranged unequally spaced over 1.86 meters on a vertical linear array. Both the transducer and hydrophone array were deployed at the bottom of the water with 20 m depth. The source-receiver range is 5.06 km. QPSK signals with a bandwidth of 4 kHz ($T = 0.25ms$) were transmitted on a carrier frequency of 17 kHz.

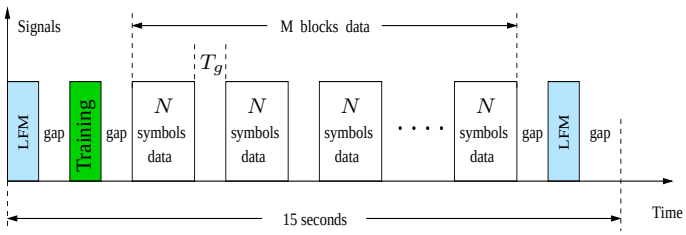

Fig. 1. Packet structure. Each packet contains M blocks of data, each data block contains one pilot symbol and $N-1$ information symbols.

The QPSK signals were partitioned in packets. The packet structure is depicted in Fig. 1. Each packet starts with an LFM signal followed by a gap, then a training block signal of 511-bit m-sequence followed by another gap, then the data package with M blocks of data, in which each block of data consists of N symbols followed by a guard time T_g seconds, finally, the packet ends up with another LFM signal and a gap. Each block of data begins with one pilot symbol for phase reference. Therefore, each packet contains $M(N-1)$ symbols of information data. The gap after the training signal is long enough so that the channel impulse response can be estimated from the training signal. The guard time T_g after each N symbols of data is sufficiently long for avoiding inter block interference. The symbol synchronization is carried out by the beginning and ending LFM signals. The gap after the ending LFM is designed to avoid inter-packet interference.

The initial channel estimation was achieved using the training signal by the proposed frequency-domain method detailed in Section III. As an example, the time-domain amplitude responses of the eight channels of the first packet is depicted in Fig. 2. The most of the channel energy is concentrated within 10 ms which corresponds to a channel length of $L = 40$ in terms of symbol-interval.

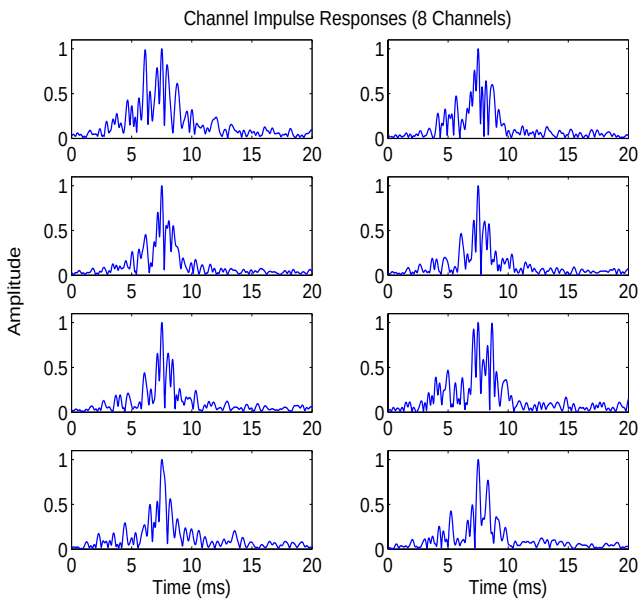

Fig. 2. A snapshot of the eight channel impulse responses of the first packet.

In this paper, we report results for the block size of $N = 512$ and $N = 1024$. When the block size $N = 512$, M was chosen to be 86, that means each packet contains $2M(N-1) = 87892$ information bits. The uncoded average bit error rates (BERs) based on 4 packets are listed in Table 1 for single channel and multiple channel receivers.

When the block size $N = 1024$, M was chosen to be 48, that means each packet contains $2M(N-1) = 98208$ information bits. The uncoded average BERs based on 4 packets are listed in Table 2 for single channel and multiple channel receivers.

As can be seen from both Tables 1 and 2, the proposed

algorithm has better BER performance for $N = 512$ than that of $N = 1024$ when the diversity channel number is less than or equal to 4. However, when the diversity channel number is larger than or equal to 5, the proposed algorithm has similar BER performance for both block size $N = 512$ and $N = 1024$.

Table 1: Average BER of single channel and multiple channel receivers for $N = 512$.

Number of Channels used	number of information bits per packet	bit error rate
1	87892	0.48
2	87892	0.075
3	87892	0.013
4	87892	0.0029
5	87892	0.0011
6	87892	4.54×10^{-4}
7	87892	7.95×10^{-5}
8	87892	6.81×10^{-5}

Table 2: Average BER of single channel and multiple channel receivers for $N = 1024$.

Number of Channels used	number of information bits per packet	bit error rate
1	98208	0.49
2	98208	0.096
3	98208	0.036
4	98208	0.013
5	98208	0.0012
6	98208	2.34×10^{-4}
7	98208	9.83×10^{-5}
8	98208	8.14×10^{-5}

VII. Conclusion

A novel frequency-domain channel estimation and equalization scheme has been proposed for single carrier underwater acoustic communication systems. The frequency-domain channel estimator utilizes a small-block training signal for initial channel estimation and converts the estimated transfer function matrices to a desired N-point frequency-domain channel transfer function matrices. Then the frequency-domain equalizer uses the linear MMSE approach to eliminate the ISI caused by the fading channel. The resulting signals are converted to time-domain and phase correction is performed with the estimated group average rotating phases. The channel transfer function matrices were re-estimated by using the detected data and received data of the current block, these re-estimated transfer function matrices were employed to equalize the next block of data in a decision-directed manner. The proposed scheme has been used to process data measured by field experiments conducted off the coast at Panama City, Florida, USA, in June 2007. In the experiment, QPSK signals with a bandwidth of 4 kHz were transmitted on a carrier frequency of 17 kHz. The experimental results have shown that the proposed frequency-domain equalizer can achieve uncoded BER on the order of 10^{-5} using $7 \sim 8$ channel diversity. It can also achieve uncoded BER between 1.2×10^{-3} and 4.5×10^{-4} for $5 \sim 6$ channel diversity systems under a typical fading channel of length 10 ms.

Acknowledgments

This work of Y. R. Zheng and C. Xiao was supported in part by the Office of Naval Research under Grant N00014-07-1-0219 and the National Science Foundation under Grant CCF-0514770. The work of T. C. Yang and W.-B. Yang was supported by the Office of Naval Research.

References

[1] M. Stojanovic, J. Catipovic, and J. Proakis, "Phase-coherent digital communicaitons for underwater acoustic channels," *IEEE J. Ocean Eng.*, vol.19, pp.100-111, Jan. 1994.

[2] T. H. Eggen, A. B. Baggeroer, and J. C. Preisig, "Communication over Doppler spread channels – Part I: channel and receiver presentation," *IEEE J. Ocean Eng.*, vol.25, pp.62-71, Jan. 2000.

[3] T. C. Yang, "Differences between passive-phase conjugation and decision-feedback equalizer for underwater acoustic communications," *IEEE J. Ocean Eng.*, vol.29, pp.472-487, April 2004.

[4] T. C. Yang, "Correlation-based decision-feedback equalizer for underwater acoustic communications," *IEEE J. Ocean Eng.*, vol.30, pp.865-880, Oct. 2005.

[5] M. Stojanovic, "Low complexity OFDM detector for underwater acoustic channels," in *Proc. Oceans'06*, 2006.

[6] B. Li, S. Zhou, M. Stojanovic, and L. Freitag, "Pilot-tone based ZP-OFDM demodulation for an underwater acoustic channel," in *Proc. Oceans'06*, 2006.

[7] D. Falconer, S. L. Ariyavisitakul, A. Benyamin-Seeyar, and B. Eidson, "Frequency domain equalization for single-carrier broadband wireless systems," *IEEE Commun. Mag.*, vol.40, no.4, pp.58-66, Apr. 2002.

[8] Y. R. Zheng and C. Xiao, "Frequency-domain channel estimation and equalization for broadband wireless communications," in *Proc. IEEE Int. Conf. Commun.*, Glasgow, Scotland, June 2007.

[9] T. Walzman and M. Schwartz, "Automatic equalization using the discrete frequency domain," *IEEE Trans. Info. Theory*, vol.IT-19, pp.57-68, Jan. 1973.

[10] B. S. Sharif, J. Neasham, O. R. Hinton, and A. E. Adams, "A computationally efficient Doppler compensation system for underwater acoustic communications," *IEEE J. Ocean Eng.*, vol.25, pp.52-61, Jan. 2000.

[11] B. Muquet, Z. Wang, G. Giannakis, M. de Courville, and P. Duhamel, "Cyclic prefix or zero padding for wireless multicarrier transmissions?" *IEEE Trans. Commun.*, vol.50, pp.2136-2148, Dec. 2002.

[12] M. V. Clark, "Adaptive frequency-domain equalization and diversity combining for broadband wireless communications," *IEEE J. Select. Areas Commun.*, vol.16, pp.1385-1395, Oct. 1998.